Available online at www.sciencedirect.com
SCIENCE DIRECT®
Chemical Engineering and Processing 43 (2004) 987–995
Chemical Engineering and Processing
www.elsevier.com/locate/cep

Volumetric mass transfer coefficients in slurry bubble columns operating in the churn-turbulent flow regime

C.O. Vandu, R. Krishna*

Department of Chemical Engineering, University of Amsterdam, Nieuwe Achtergracht 166, NL-1018 WV Amsterdam, The Netherlands

Received 16 June 2003; received in revised form 18 September 2003; accepted 29 September 2003

Available online 3 December 2003

Abstract

We report the results of an extensive experimental study of the gas hold-up, ε, and volumetric mass transfer coefficient, $k_L a$, in bubble columns operated at ambient temperature and pressure conditions. The superficial gas velocity U was varied in the range 0–0.4 m/s, spanning both the homogeneous and churn-turbulent flow regimes. Air was used as the gas phase in all cases. Three different measurement campaigns were carried out.

In the first campaign the influence of liquid properties (viscosity, surface tension) were investigated in a column of 0.1 m diameter, equipped with a sieve plate distributor with 0.5 mm holes. Four different liquids were investigated: water, tetradecane, paraffin oil and Tellus oil, with viscosities ranging from 1 to 75 mPa s. The gas hold-up ε_G in these systems vary significantly. The volumetric mass transfer coefficient, $k_L a$, closely follows the trend in gas hold-up. For the churn-turbulent regime of operation, i.e. $U > 0.08$ m/s, the value of $k_L a/\varepsilon_G$ is found to be practically independent of U; the value of this parameter is found to depend on the liquid phase Schmidt number, showing a $Sc^{-1/3}$ dependence.

In the second campaign, we investigated the influence of catalyst particles addition (porous silica, mean diameter = 38 μm) to the liquid phase (water and tetradecane), with slurry concentrations varying up to 25 vol.%. With increasing slurry concentrations, ε_G is significantly reduced due to enhanced bubble coalescence and for high slurry concentrations, the "small" bubbles are almost completely destroyed. For $U > 0.08$ m/s, the value of $k_L a/\varepsilon_G$ is again found to be practically independent of U; this parameter is however significantly lowered with increased catalyst concentrations, due to increase in the size of the "large" bubbles.

In the third campaign, the influence of increasing column diameter D_T was investigated by experiments with water and Tellus oil. For both systems, $k_L a/\varepsilon_G$ shows a slight increase with D_T in the churn-turbulent regime. This increase is due to increased liquid circulations with increasing scale, leading enhanced bubble split up. Our studies provide a simple method for estimation of $k_L a$ in industrial size slurry bubble columns operating in the churn-turbulent flow regime.

Keywords: Bubble columns; Slurries; Mass transfer coefficient; Heterogeneous flow regime; Scale effects

1. Introduction

Bubble columns are widely used in industry for carrying out a variety of chemical reactions such as hydrogenations, chlorinations, oxidations and the Fischer–Tropsch synthesis [1]. In bubble column slurry reactors catalyst particle sizes smaller than say 100 μm can be used, thus eliminating intra-particle diffusion resistances. These catalyst particles are held in suspension due to the liquid circulations caused by the rising gas bubbles. For the highly exothermic Fischer–Tropsch synthesis, the slurry bubble column is the favoured reactor choice and high reactor productivities are achieved by use of high slurry concentrations (up to 25 vol.%) in columns approaching 10 m in diameter and height of 40 m [2–4], operating at high superficial gas velocities, U, in the 0.3–0.4 m/s range. While there have been several experimental studies on mass transfer in slurry bubble columns (for literature surveys see Inga and Morsi [5] and Behkish et al. [6]), most of the published work is restricted to values $U < 0.1$ m/s, in columns of diameter $D_T < 0.1$ m, with low slurry concentrations. We know of no reliable procedures for estimation of the volumetric mass transfer coefficient, $k_L a$, in large diameter slurry bubble columns operating at high slurry concentrations *and* high U-values in the churn-turbulent regime. The major objective of this paper is to attempt to fill this gap in our knowledge and to provide a

* Corresponding author. Tel.: +31-20-525-7007; fax: +31-20-525-5604.
E-mail address: krishna@science.uva.nl (R. Krishna).

0255-2701/$ – see front matter © 2003 Elsevier B.V. All rights reserved.
doi:10.1016/j.cep.2003.09.007

practical and simple approach to estimating $k_L a$ values for industrial size slurry reactors. To reach our objective we carried out a systematic and comprehensive program of experiments with varying liquid properties, slurry concentrations and column diameters.

2. Experimental

Experiments were carried out in polyacrylate columns of 0.1, 0.15, 0.38 and 0.63 m diameters. The experimental set-up for the 0.1 m column is shown in Fig. 1; this was typical of all set-ups used. The 0.1, 0.15 and 0.38 m diameter columns were equipped with brass sieve plate distributors with 0.5 mm diameter holes. The 0.63 m diameter column was equipped with a spider shaped sparger (see inset to Fig. 1). Details of the distributors are specified in Table 1. The rate of air flow into each column was controlled by the use of one or more pre-calibrated rotametres aligned in parallel. Nitrogen flow (employed for stripping out dissolved oxygen) was controlled by the use of manually operated control valves connected to each of the bubble columns. Pressure taps were installed along the height of the columns for the determination of gas hold-up ε_G.

Four different liquids were used in the experiments: water, tetradecane, paraffin oil, and Tellus oil in the experiments; the properties are specified in Table 2. The solid phase used consisted of porous silica particles (properties specified in Table 3). The solids concentration ε_s, is expressed as the volume fraction of solids in gas-free slurry with the pore volume of the particles (liquid filled during operation) being counted as being part of the solid phase. The temperature used in the experiments corresponded to ambient conditions, about 293 K.

Table 1
Details of distributors used in the column

Column diameter (m)	Type of distributor	Hole diameter (m)	Number of holes
0.1	Brass sieve plate	0.5	199, on triangular pitch
0.15	Brass sieve plate	0.5	625, on triangular pitch
0.38	Brass sieve plate	0.5	2750, on triangular pitch
0.63	Spider shaped sparger	2.5	64

Table 2
Properties of liquids used

Liquid	Density, ρ_L (kg/m^3)	Viscosity, μ_L (mPa s)	Surface tension, σ (mN/m)	Oxygen diffusivity in liquid, $\mathcal{D}_L$ (10^{-9} m^2/s)
Water	998	1	72	2.11
Tetradecane	763	2.2	27	4.11
Paraffin oil	795	2.9	28	3.69
Tellus oil	862	75	28	1.02
Ethanol	798	1.27	23	2.02

Ethanol was used only for determination of the sensor constant of the oxygen probe.

Table 3
Properties of silica catalyst particles used

Property	
Skeletal density (kg/m^3)	2100
Pore volume (ml/g)	1.05
Particle size	10%, <27 μm; 50%, <38 μm; 90%, <47 μm

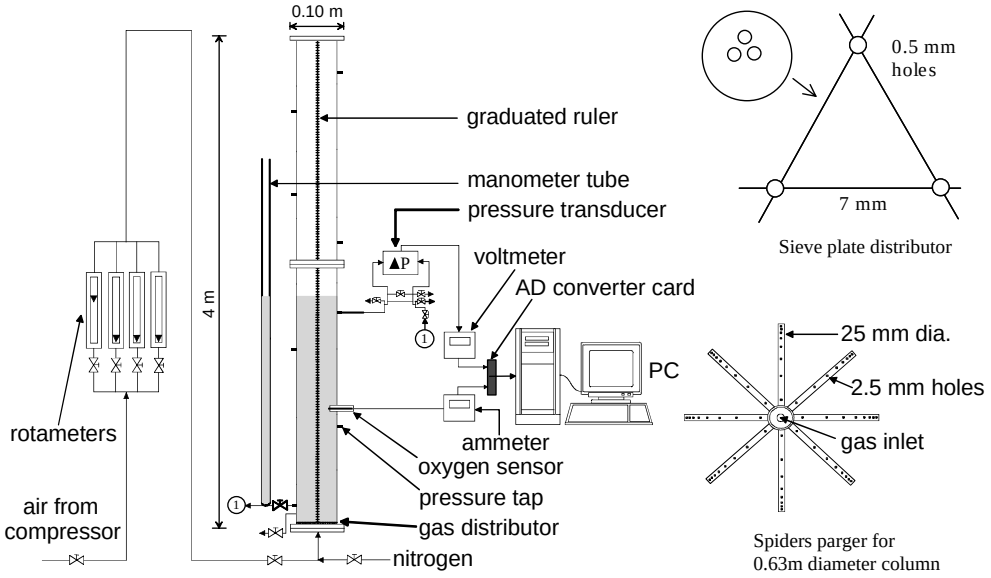

Fig. 1. Typical experimental set-up for the 0.1 m diameter column. The inset on the right shows the two types of distributors used. The spider type of distributor was used in the 0.63 m diameter column. Further details are available on our website: http://ct-cr4.chem.uva.nl/BubbleColumnExpt/.

Table 4
Experimental systems studied

Column diameter, D_T (m)	Liquid	Solids concentration, ε_s	Height of ungassed liquid, H_0 (m)	ε_G measurement technique
0.1	Water	0	1.6	Pressure sensor
0.1	Water	0.136	1.61	Visual
0.1	Water	0.213	1.61	Visual
0.1	Paraffin oil	0	1.44 and 1.59	Pressure sensor
0.1	Tetradecane	0	1.22	Visual
0.1	Tetradecane	0.045	1.24	Visual
0.1	Tetradecane	0.15	1.27	Visual
0.1	Tetradecane	0.25	1.3	Visual
0.1	Tellus oil	0	1.3	Visual
0.15	Water	0	1.6	Pressure sensor
0.38	Water	0	1.6	Pressure sensor
0.38	Tellus oil	0	1.73	Visual
0.63	Water	0	2.18	Pressure sensor

The gas hold-up was determined either by the use of the pressure taps installed along the height of the bubble columns or by visual measurements (refer to Table 4). In the first method, two pressure taps, one of which was positioned close to the column base and the other close to the clear liquid height, were used. The taps were connected to pressure ports on a Validyne DP15 pressure transducer, which was in turn coupled to a PC via an analogue-to-digital (AD) converter system consisting of the pressure transducer, a voltmeter and an analogue-to-digital converter card on the PC. To determine the gas hold-up in each experiment, the gas flow rate was adjusted using one rotametre at a time. Sufficient time was given for steady state to be reached in each column after which the increase in liquid pressure at the higher of the two pressure taps used was recorded. The measured pressure signals, obtained in the form of voltage readings were interpreted to obtain information on the gas hold-ups. In the second method, gas hold-up values were obtained by visual observation. In this case, the total gas hold-up, ε_G is defined as

$$\varepsilon_G = \frac{H - H_0}{H} \tag{1}$$

where H_0 is the ungassed column height and H is the column dispersion height due to the presence of gas bubbles.

3. Experimental determination of $k_L a$

The volumetric mass transfer coefficient $k_L a$ was determined by means of a dynamic oxygen absorption technique [7]. An oxygen electrode (*Yellow Springs Incorporated* Model 5331) was used to measure the change in dissolved oxygen concentration. Readings given by the electrode were fed to the PC via an ammeter and the AD converter card. The change in dissolved oxygen concentration was reflected as a change in electrical current displayed on the ammeter.

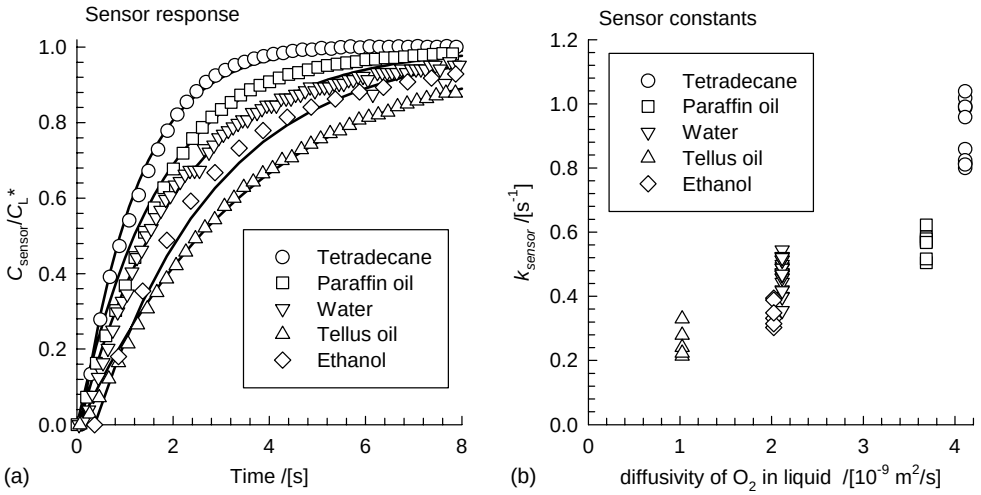

Fig. 2. (a) Dynamic oxygen sensor responses for liquids employed in this study, and ethanol. The model fits using Eq. (3) are shown by continuous lines and k_{sensor} values obtained are 0.86, 0.58, 0.47,0.28 and 0.39 s^{-1} for tetradecane, paraffin oil, water, Tellus oil and ethanol, respectively. (b) Relationship between k_{sensor} and estimated liquid phase diffusivity of oxygen.

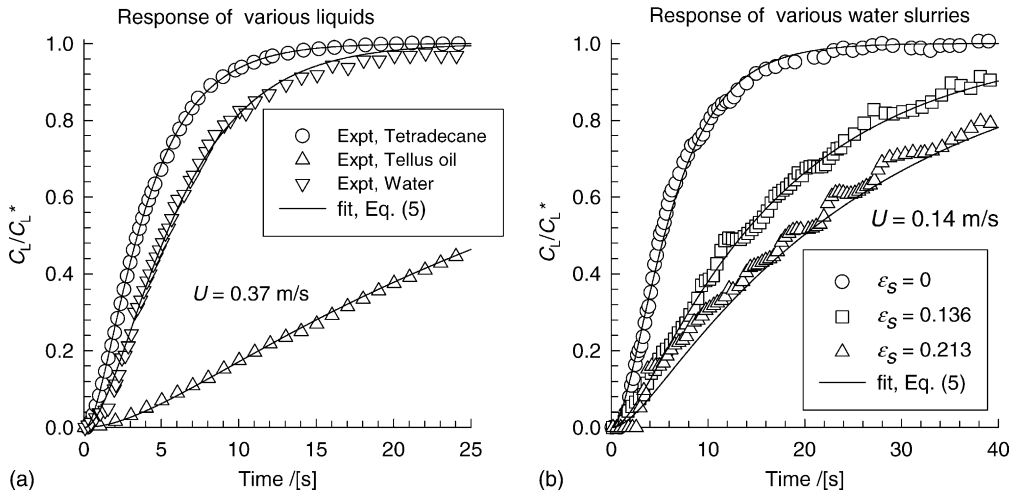

Fig. 3. (a) Oxygen absorption dynamics with tetradecane, water and Tellus oil as liquids in the 0.1 m diameter column at $U = 0.37$ m/s. The values of k_La_L, resulting from the fits using Eq. (5) and shown by continuous lines are 0.323, 0.238 and 0.03 s^{-1}, respectively. (b) Oxygen absorption dynamics for air–water–silica system in the 0.1 m diameter column at $U = 0.14$ m/s with varying slurry concentrations. k_La_L values resulting from the fits using Eq. (5) are 0.223, 0.061 and 0.038 s^{-1} for $\varepsilon_s = 0$, 0.136 and 0.213, respectively.

Prior to conducting experiments in each of the systems investigated, the time constant of the oxygen sensor was determined at the same temperature as used in the experiments, i.e. 293 K. Every time this was done, the membrane surrounding the tip of the electrode was changed. The sensor constant value corresponds to an inherent delay in readings obtained as a result of the fact that the oxygen sensor has a finite response time. In determining the sensor constant, two continuously stirred glass beakers were used, the first containing the particular liquid employed for a given set of experiments, and the other, the liquid (or slurry with silica particles in the same ratio as was present in the bubble column). Nitrogen was continuously bubbled into the first beaker and air into the other, such that the liquid phases in both beakers became completely saturated with dissolved gas over time. The sensor was first placed in the nitrogen-saturated liquid and after registering a negligible oxygen concentration, was instantaneously transferred to the oxygen-saturated liquid.

Assuming perfect mixing in the liquid phase within each beaker, the oxygen concentration value indicated by the sensor, C_{sensor} is given by

$$\frac{dC_{sensor}}{dt} = k_{sensor}(C_L^* - C_{sensor}) \quad (2)$$

where k_{sensor} is the sensor time constant. Integrating Eq. (2) gives

$$\frac{C_{sensor}}{C_L^*} = 1 - e^{-k_{sensor}t} \quad (3)$$

Fig. 2(a) shows typical sensor responses for the various liquids employed which included also ethanol. These correspond to the maximum rates of oxygen detection by the sensor for each liquid. It is apparent from these curves that the value of k_{sensor} is dependent on liquid properties. Fitting Eq. (3) to these curves gives k_{sensor} values of 0.86, 0.58, 0.47, 0.28 and 0.39 s^{-1} for tetradecane, paraffin oil,

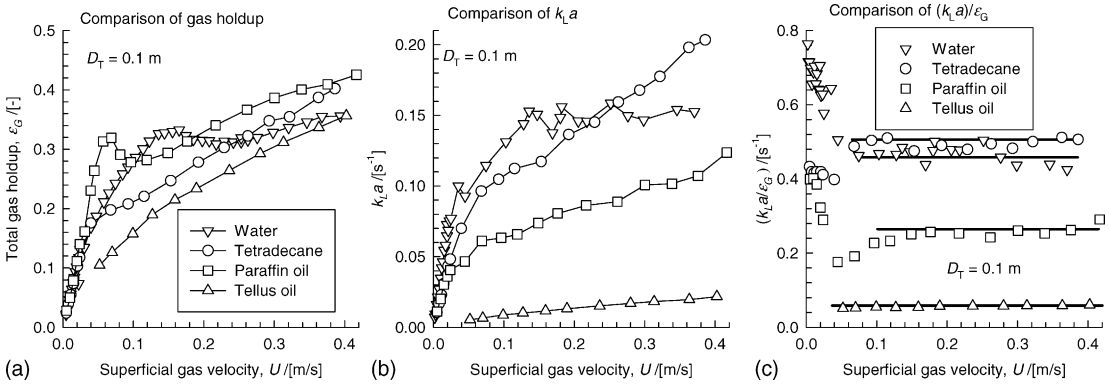

Fig. 4. Influence of liquid properties on (a) gas hold-up, ε_G; (b) volumetric mass transfer coefficient, k_La and (c) k_La/ε_G. Variation with superficial gas velocity, U, for water, tetradecane, paraffin oil, and Tellus oil systems in the 0.1 m diameter column.

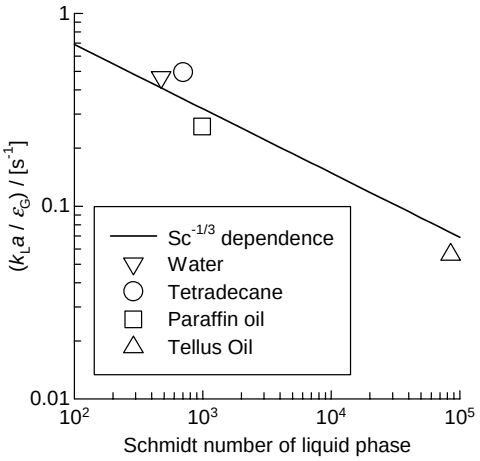

Fig. 5. Influence of liquid phase Schmidt number on the "plateau" values of k_La/ε_G in the churn-turbulent flow regime.

water, Tellus oil and ethanol, respectively, values typical of the averages obtained for each liquid. Using literature correlations [8] we estimated the liquid phase diffusivity of oxygen, $\mathcal{D}_L$, for each of the liquids employed (using the Wilke–Chang correlation for oxygen diffusivities in water and ethanol, and Hayduk–Minhas for oxygen diffusivities in paraffin oil, tetradecane and Tellus oil) (see Table 2). The sensor constant is found to depend on the $\mathcal{D}_L$ in the liquid phase (see Fig. 2(b)). It appears that k_{sensor} is not entirely a sensor property but is also dictated by oxygen diffusion through a stagnant liquid layer surrounding the oxygen sensor.

For determination of k_La in the bubble columns, dissolved oxygen was stripped from the liquid phase in each column to a negligible concentration by the use of nitrogen sparged through the gas distributor. After the stripping operation is complete and the nitrogen bubbles have escaped, a step input of air was then introduced into the column and the dynamic response was monitored. Sufficient time was given in each experimental run for the oxygen saturation concentration in the liquid, C_L^* to be reached. The dynamic response was found not to depend on the sensor placement location in the column and the assumption of completely mixed liquid phase is justified for the range of column diameters studied in this work. Also, the oxygen solubility in the various liquids was low enough to ensure that the variation of the oxygen concentration in the gas phase, and its dynamics, had no influence on the oxygen uptake characteristics. Based on the assumptions that the liquid is perfectly mixed and oxygen depletion from the gas bubbles is negligible, the rate of oxygen uptake is described by

$$\frac{dC_L}{dt} = k_La_L(C_L^* - C_L) \quad (4)$$

where k_La_L is the volumetric mass transfer coefficient per unit volume of *liquid* in the bubble column. Analytical

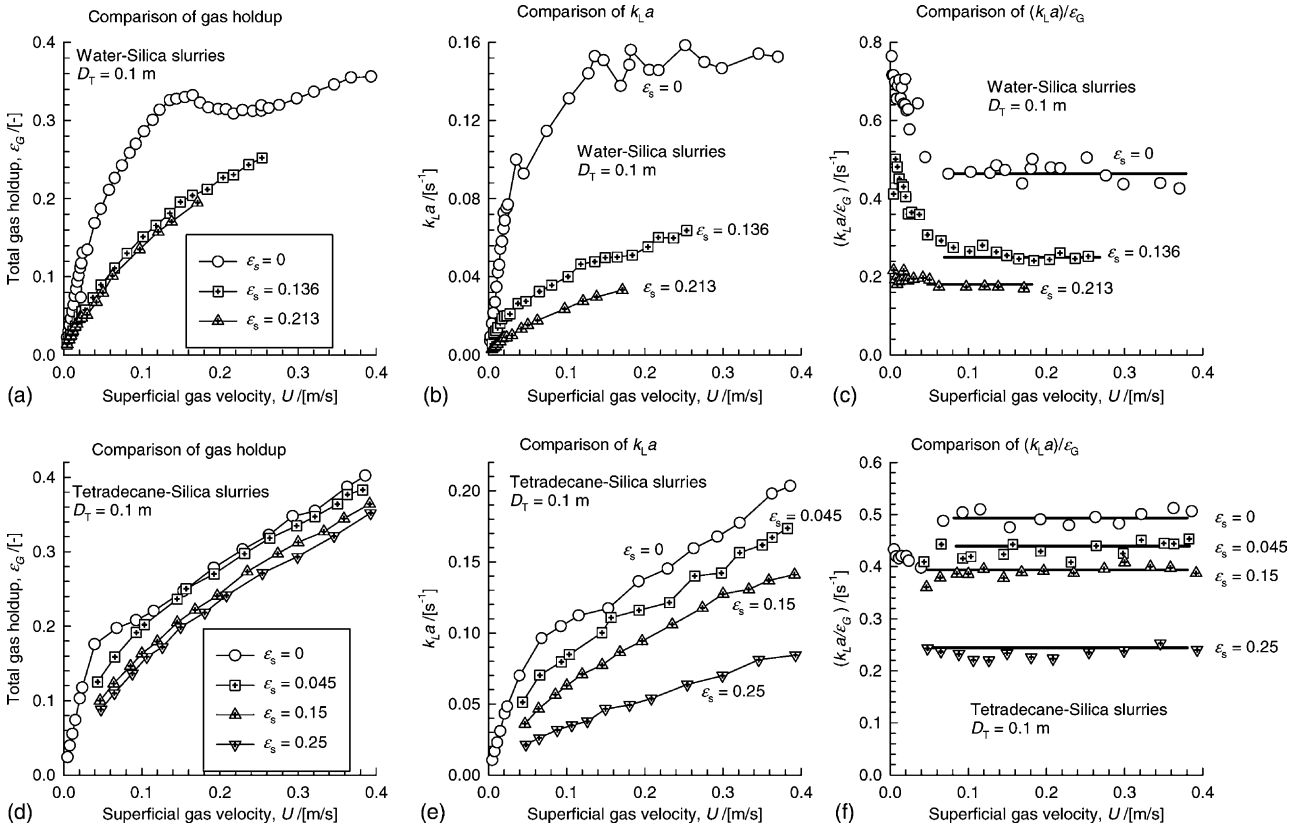

Fig. 6. Influence of slurry concentrations on hold-up and mass transfer in water (a–c) and tetradecane (d–f) systems in a 0.1 m diameter column.

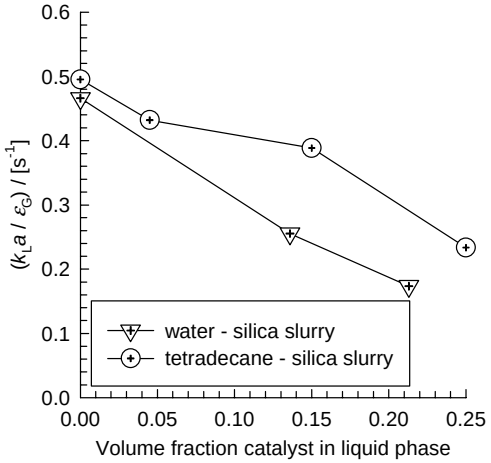

Fig. 7. Influence of slurry concentration on the "plateau" values of k_La/ε_G in the churn-turbulent flow regime for water and tetradecane slurries.

solution of Eq. (4), along with the sensor dynamics given by Eq. (2), yields [9]

$$\frac{C_L}{C_L^*} = 1 - \frac{1}{k_{sensor} - k_La_L}[k_{sensor}e^{-k_La_Lt} - k_La_Le^{-k_{sensor}t}] \quad (5)$$

The volumetric mass transfer coefficient per unit volume of *dispersion* (gas + liquid + solid), k_La is obtained from

$$k_La = k_La_L(1-\varepsilon_G)(1-f_s\varepsilon_s) \quad (6)$$

where f_s is the volume fraction of the solid particles due to the solid skeleton structure (i.e. subtracting the solid pore volume contribution). Gas–liquid mass transfer can occur in the pores of the solid particles, which become filled with liquid during experiments, making it necessary to account for this contribution. For pure liquids, $k_La = k_La_L(1-\varepsilon_G)$.

Fig. 3(a) shows the oxygen absorption dynamics experimental data at $U = 0.37$ m/s when different liquids were employed in the 0.1 m diameter column. The fitted values of k_La_L obtained are 0.323, 0.238 and 0.03 s^{-1}, respectively, for tetradecane, water and Tellus oil; the fits are shown by the continuous lines. Fig. 3(b) shows oxygen absorption dynamics for air–water–silica system in the 0.1 m diameter column operating at $U = 0.14$ m/s. By comparing the sensor dynamics (Fig. 2) and the oxygen absorption dynamics in the bubble column (Fig. 3) we conclude that the sensor response is fast enough not to dominate the oxygen absorption dynamics in the bubble column. So the influence of the k_{sensor} correction to the fitted k_La_L values was small in all the experiments; even so, this correction was rigorously applied in all cases.

Further details of the experimental set-up and measurement techniques, including photographs and video recordings are available on our website: http://ct-cr4.chem.uva.nl/BubbleColumnExpt/.

4. Influence of liquid properties on k_La

Fig. 4 shows the variation of (a) gas hold-up, ε_G (b) volumetric mass transfer coefficient, k_La, and (c) k_La/ε_G with superficial gas velocity U in a 0.1 m diameter column operating with four different liquids. For liquids with low viscosities, water, tetradecane and paraffin oil, Fig. 4(a) shows the existence of both homogeneous and heterogeneous flow regimes, with regime transition taking place at values of U in the region of 0.04 m/s. Paraffin oil, which consists of a mixture of linear hydrocarbons, shows a strong tendency to foam at low gas velocities and the ε_G–U curve shows a sharp maximum at $U = 0.06$ m/s. With Tellus oil, a kind of motor oil with $\mu_L = 75$ mPa s, as the liquid phase the homogeneous regime of operation is virtually non-existent and large fast rising bubbles appear even at low values of U. Dynamic gas disengagement experiments have confirmed that for Tellus oil the dispersion consists predominantly of large fast-rising bubbles [10]. The k_La values (see Fig. 4(b)) largely follow the trend in ε_G, except that no sharp maxima are detected. Fig. 4(c) shows the values of k_La/ε_G, which represents the volumetric mass transfer coefficient *per unit volume of dispersed gas bubbles* for the four different liquids. We see that for values of U exceeding about 0.08 m/s,

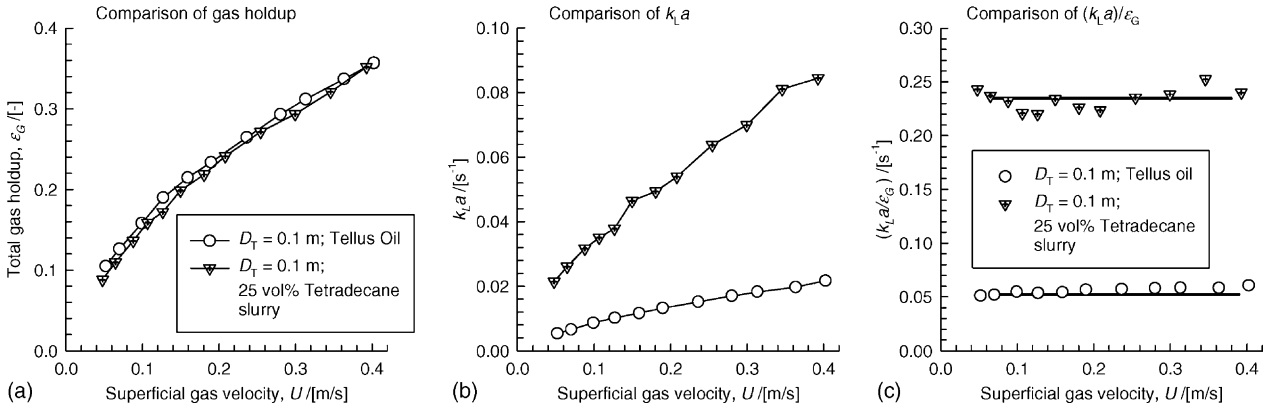

Fig. 8. (a–c) Comparison of the hydrodynamics and mass transfer in Tellus oil and 25 vol.% tetradecane slurry systems.

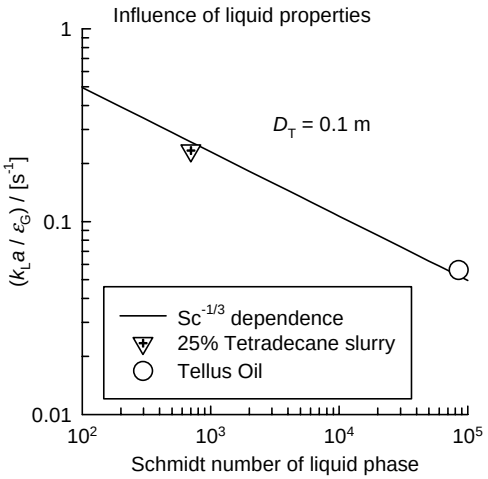

Fig. 9. Influence of liquid phase Schmidt number on the "plateau" value of k_La/ε_G in the churn-turbulent flow regime for Tellus oil and 25 vol.% tetradecane slurry systems.

i.e. well and truly heterogeneous regime, k_La/ε_G is virtually independent of U. These "plateau" values are indicated by the thick horizontal lines in Fig. 4(c). The "plateau" values of k_La/ε_G show a dependence on the liquid phase Schmidt number, following $Sc^{-1/3}$ (see Fig. 5). The $Sc^{-1/3}$ dependence is typical of boundary layer mass transfer theories for k_L.

5. Influence of increased slurry concentration on k_La

Fig. 6 summarises the gas hold-up and mass transfer data for water and tetradecane slurries, as measured in the 0.1 m diameter column. Addition of catalyst particles tends to reduce the gas hold-up to a significant extent (see Fig. 6(a) and (d)). The results shown in Fig. 6(a) and (d) are consistent with our earlier work on gas hold-up in paraffin oil slurries [11]. For both water and tetradecane slurry systems, the homogeneous regime of operation is virtually non-existent for high slurry concentrations. The influence of catalyst addition tends to cause a more significant reduction in the k_La and k_La/ε_G values (see Fig. 6(b), (c), (e) and (f)). The "plateau" values of k_La/ε_G are plotted in Fig. 7 for water and tetradecane slurries. The strong decrease in the k_La/ε_G with increasing values of ε_s must be attributed to the increase in the size of the fast rising large bubbles in the churn-turbulent regime. It also appears that the bubble size for water slurries is larger than for tetradecane slurries.

Visually, the hydrodynamics of highly concentrated slurries appears analogous to that of the highly viscous Tellus

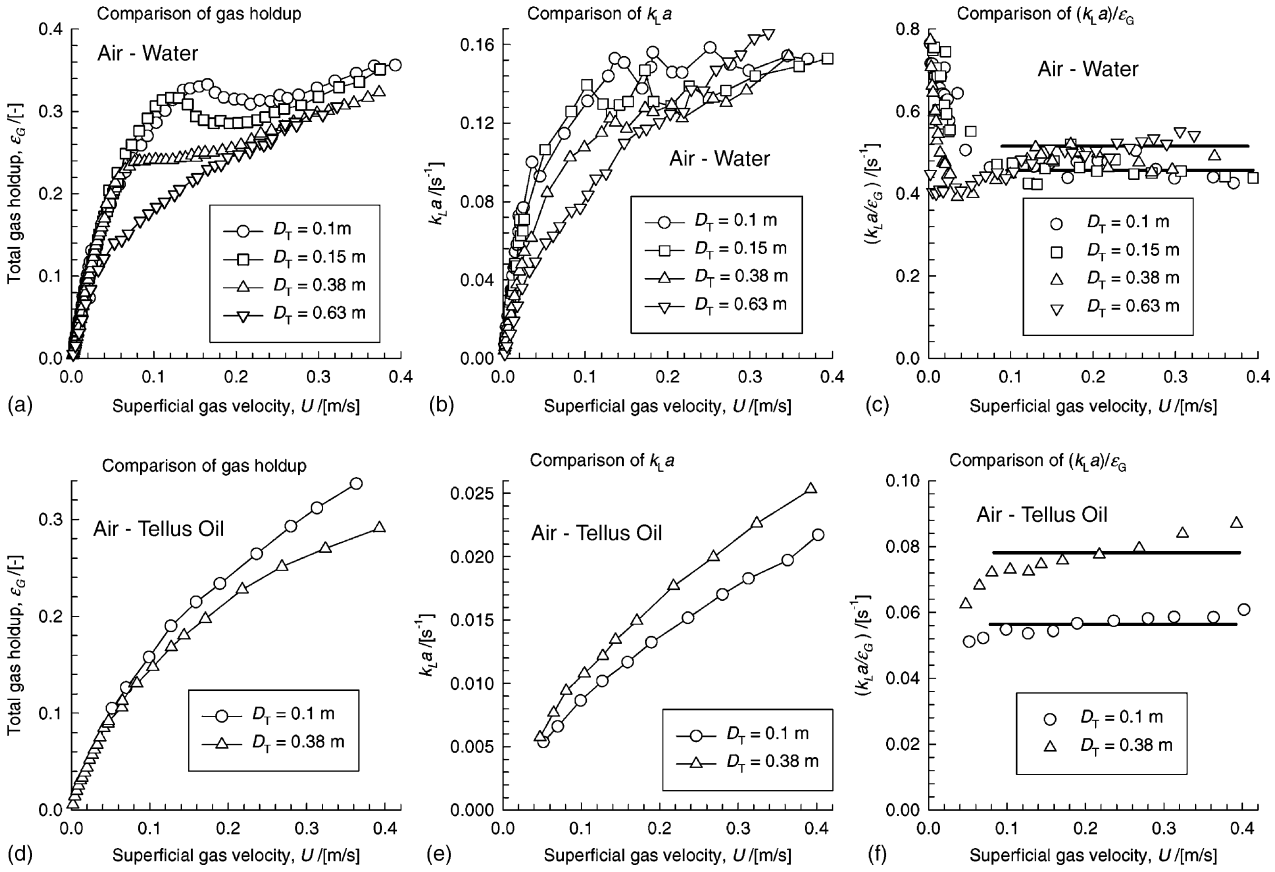

Fig. 10. Influence of column diameter on hold-up and mass transfer in water (a–c) and Tellus oil (d–f) systems.

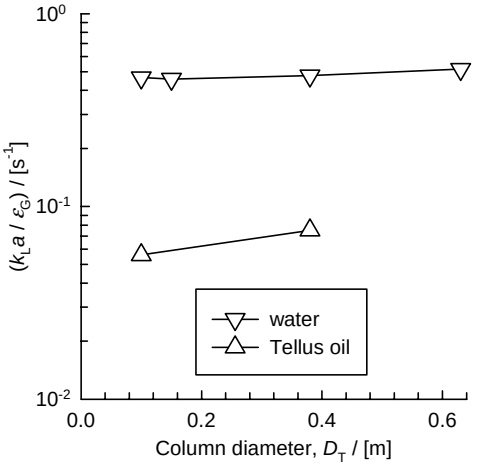

Fig. 11. Influence of column diameter on the "plateau" value of $k_L a/\varepsilon_G$ in the churn-turbulent flow regime.

oil; we had also made this observation in an earlier study [10] when comparing the hold-up of Tellus oil with that of paraffin oil slurries. In Fig. 8, we compare the hydrodynamics and mass transfer of Tellus oil with that of 25 vol.% tetradecane slurry. The gas hold-up of these two systems show an almost identical variation with U (see Fig. 8(a)). This points to identical bubble sizes and bubble rise velocities in these two systems, a conclusion underlined by dynamic gas disengagement experiments [10].

The $k_L a$ and $k_L a/\varepsilon_G$ values of Tellus oil and 25 vol.% tetradecane slurry systems are compared in Fig. 8(b) and (c). The significantly lower "plateau" value of $k_L a/\varepsilon_G$ for Tellus oil when compared with 25 vol.% tetradecane slurry, is to be attributed to the liquid phase properties, encapsulated in the Schmidt number, Sc. Fig. 9 demonstrates $k_L a/\varepsilon_G$ for Tellus oil and 25 vol.% tetradecane slurry systems follow the $Sc^{-1/3}$ typical of boundary layer mass transfer theory. Fig. 9 would strongly suggest that the large bubble sizes in viscous Tellus oil system are identical to that for concentrated tetradecane slurry.

6. Influence of column diameter on $k_L a$

Fig. 10 shows the influence of varying column diameter on the hydrodynamics and mass transfer in water and Tellus oil systems. With water as the liquid phase, the $k_L a/\varepsilon_G$ for columns of 0.1, 0.15 and 0.38 m diameter are virtually the same; Fig. 10(c). For the 0.63 m diameter column, equipped with sparger leading to *poorer gas distribution*, the slightly *higher* $k_L a/\varepsilon_G$ measured experimentally appears to be paradoxical. The only rational explanation is that the increased liquid recirculations in the larger diameter 0.63 m diameter column, measured in earlier work [12], enhances the splitting up process of large bubbles. For the Tellus oil system, which consists predominantly of large bubbles, we would expect the large bubble splitting process to be of greater significance. Indeed we see in Fig 10(e) and (f) that *both* $k_L a$ and $k_L a/\varepsilon_G$ appear to increase with increasing column diameter. This result validates the conclusion that increased liquid recirculations in larger diameter columns cause a reduction in large bubble sizes. Fig. 11 shows that the "plateau" values of $k_L a/\varepsilon_G$ in the churn-turbulent regime shows a slight increase with column diameter.

7. Conclusions

The following major conclusions can be drawn from this work.

(1) For all systems studied, the volumetric mass transfer coefficient per unit volume of dispersed gas bubbles, $k_L a/\varepsilon_G$, is practically independent of the superficial gas velocity in the churn-turbulent regime, i.e. for $U > 0.08$ m/s.
(2) For pure liquids, $k_L a/\varepsilon_G$ in the churn-turbulent regime shows a $Sc^{-1/3}$ dependence where Sc is the liquid phase Schmidt number.
(3) The $k_L a/\varepsilon_G$ values are significantly reduced with increased solids concentration in slurries, pointing to larger bubble sizes caused by enhanced coalescence promotion due to presence of solids.
(4) The $k_L a/\varepsilon_G$ appear to show a slight but distinct increase with column diameter. This is caused by enhanced bubble splitting due to liquid recirculations that increase sharply with increased column diameter.

From a scale up point of view, it appears that the key to successful scale up is the estimation of the gas hold-up ε_G. The $k_L a$ values in the churn-turbulent regime for slurry bubble columns can be estimated by introducing appropriate corrections for the liquid properties (via the Schmidt number) and slurry concentrations.

Appendix A. Nomenclature

a	gas–liquid interfacial area per unit dispersion volume (m^{-1})
a_L	gas–liquid interfacial area per unit liquid volume (m^{-1})
C_L	oxygen concentration in the liquid phase, arbitrary units
C_L^*	saturation concentration of oxygen in liquid, arbitrary units
C_{sensor}	liquid phase oxygen concentration given by sensor, arbitrary units
$Đ_L$	diffusivity of oxygen in the liquid phase (m^2/s)
D_T	column diameter (m)
f_s	volume fraction of catalyst that is (non-porous) skeleton (dimensionless)

H	dispersion height in the column (m)
H_0	height of ungassed column (m)
k_L	liquid-side mass transfer coefficient (m/s)
k_{sensor}	sensor time constant (s^{-1})
Sc	liquid phase Schmidt number, $Sc = (\mu_L/\rho_L \mathcal{D}_L)$ (dimensionless)
t	time (s)
U	superficial gas velocity (m/s)

Greek letters

ε_G	total gas hold-up (dimensionless)
μ_L	liquid viscosity (Pa s)
ρ_L	liquid density ($kg\,m^{-3}$)
σ	surface tension ($N\,m^{-1}$)

Subscripts

b	referring to bubbles
G	referring to gas phase
L	referring to liquid
T	tower or column

References

[1] W.D. Deckwer, Bubble Column Reactors, Wiley, New York, NY, 1992.

[2] R. Krishna, J.M. van Baten, M.I. Urseanu, J. Ellenberger, Design and scale up of a bubble column slurry reactor for Fischer–Tropsch synthesis, Chem. Eng. Sci. 56 (2001) 537–545.

[3] R. Krishna, A scale-up strategy for a commercial scale bubble column slurry reactor for Fischer–Tropsch synthesis, Oil Gas Sci. Technol. 55 (2000) 359–393.

[4] C. Maretto, R. Krishna, Modelling of a bubble column slurry reactor for Fischer–Tropsch synthesis, Catal. Today 52 (1999) 279–289.

[5] J.R. Inga, B.I. Morsi, Effect of operating variables on the gas hold-up in a large-scale slurry bubble column reactor operating with an organic liquid mixture, Ind. Eng. Chem. Res. 38 (1999) 928–937.

[6] A. Behkish, Z.W. Men, J.R. Inga, B.I. Morsi, Mass transfer characteristics in a large-scale slurry bubble column reactor with organic liquid mixtures, Chem. Eng. Sci. 57 (2002) 3307–3324.

[7] M. Letzel, A. Stankiewicz, Gas hold-up and mass transfer in gas-lift reactors operated at elevated pressures, Chem. Eng. Sci. 54 (1999) 5153–5157.

[8] B.E. Poling, J.M. Prausnitz, J.P. O'Connell, The Properties of Gases and Liquids, fifth ed., McGraw-Hill, New York, NY, 2001.

[9] H.M. Letzel, J.C. Schouten, R. Krishna, C.M. van den Bleek, Gas hold-up and mass transfer in bubble column reactors operated at elevated pressure, Chem. Eng. Sci. 54 (1999) 2237–2246.

[10] R. Krishna, M.I. Urseanu, J.W.A. de Swart, J. Ellenberger, Gas hold-up in bubble columns: operation with concentrated slurries versus high viscosity liquid, Can. J. Chem. Eng. 78 (2000) 442–448.

[11] R. Krishna, J.W.A. de Swart, J. Ellenberger, G.B. Martina, C. Maretto, Gas hold-up in slurry bubble columns: effect of column diameter and slurry concentrations, AIChE J. 43 (1997) 311–316.

[12] R. Krishna, M.I. Urseanu, J.M. van Baten, J. Ellenberger, Influence of scale on the hydrodynamics of bubble columns operating in the churn-turbulent regime: experiments vs. Eulerian simulations, Chem. Eng. Sci. 54 (1999) 4903–4911.